Earthquakes and Structures, *Vol. 15, No. 4 (2018) 431-441*
DOI: https://doi.org/10.12989/eas.2018.15.4.431

Fragility assessment of RC bridges using numerical analysis and artificial neural networks

Mehran S. Razzaghi*[1], Mehrdad Safarkhanlou[1], Araliya Mosleh[2] and Parisa Hosseini[1]

[1]*Department of Civil Engineering, Qazvin Branch, Islamic Azad University, Qazvin, Iran*
[2]*CONSTRUCT-LESE, Department of Civil Engineering, Faculty of Engineering, University of Porto, 4200-465 Porto, Portugal*

(Received November 22, 2017, Revised May 15, 2018, Accepted July 16, 2018)

Abstract. This study provides fragility-based assessment of seismic performance of reinforced concrete bridges. Seismic fragility curves were created using nonlinear analysis (NA) and artificial neural networks (ANNs). Nonlinear response history analyses were performed, in order to calculate the seismic performances of the bridges. To this end, 306 bridge-earthquake cases were considered. A multi-layered perceptron (MLP) neural network was implemented to predict the seismic performances of the selected bridges. The MLP neural networks considered herein consist of an input layer with four input vectors; two hidden layers and an output vector. In order to train ANNs, 70% of the numerical results were selected, and the remained 30% were employed for testing the reliability and validation of ANNs. Several structures of MLP neural networks were examined in order to obtain suitable neural networks. After achieving the most proper structure of neural network, it was used for generating new data. A total number of 600 new bridge-earthquake cases were generated based on neural simulation. Finally, probabilistic seismic safety analyses were conducted. Herein, fragility curves were developed using numerical results, neural predictions and the combination of numerical and neural data. Results of this study revealed that ANNs are suitable tools for predicting seismic performances of RC bridges. It was also shown that yield stresses of the reinforcements is one of the important sources of uncertainty in fragility analysis of RC bridges.

Keywords: fragility curves; seismic performance; artificial neural network; bridge

1. Introduction

Bridges are one of the important components in the transportation networks. They play a fundamental role to maintain fast and smooth communication systems prior to and after the seismic disaster. Bridge damages during the earthquakes can lead to noticeable physical and economic impacts to the transportation system. A vast majority of highway bridges around the world do not meet the seismic detailing requirements imposed by current codes and guidelines (Caltrans 2013).

In the past decades, several highway bridges have experienced remarkable damages due to major earthquakes (e.g., 1989 Loma Prieta, 1994 Northridge in the US and 1995 Kobe earthquake in Japan).

Field observations following the above-mentioned earthquakes revealed that highway bridges are seismically vulnerable. Hence, evaluation of the seismic vulnerability of the highway bridges is an important task in seismic risk management of transportation systems.

The available procedure for seismic risk assessment (Whitman *et al.* 1975) revealed the importance of probabilistic evaluation of seismic vulnerability of structures. Deriving fragility functions is one of the common methods for assessing the seismic performance of structures. Seismic fragility curves provide a probabilistic field to evaluate the seismic performance of a particular structure versus severity of ground motion (Hwang *et al.* 2001, Billah and Alam 2015). In 1991, the concept of using a continuous function for evaluating the seismic performance was proposed by ATC 25 (ATC 1991) for the first time by introducing continuous damage function. Subsequently in 1997, a commercial-off-the-shelf loss and risk assessment software package based on the geographical information system (GIS) was released by FEMA, so-called HAZUS (HAZUS 1997). During the recent years, fragility curves have evolved as significant tools for stake holders and decision makers by providing a probabilistic approach for assessment of the seismic risk. Although there are at least four approaches for development of fragility curves (judgmental, empirical, analytical and hybrid), most of the researchers have used analytical approaches for fragility analysis of the bridges (Shinozuka *et al.* 2003, Moschonas *et al.* 2009, Huo and Zhang 2012, Padgett *et al.* 2013, Yazgan 2015, Mosleh *et al.* 2018a). Various analytical methods can be carried out for developing analytical fragility curves. Nonlinear static analysis (Monti and Nisticò 2002, Banerjee and Shinozuka 2007), nonlinear response history analysis (Hwang *et al.* 2001, Choi *et al.* 2004, Mosleh *et al.* 2016a, Mosleh *et al.* 2018b) and incremental dynamic analysis (Billah *et al.* 2012, Billah and Alam 2016) are some of the common methods for development of analytical fragility functions. It should be noted that nonlinear response history analysis is known as the most reliable method of developing fragility curves; but it is the most

*Corresponding author, Assistant Professor
E-mail: razzaghi.m@gmail.com

ISSN: 2092-7614 (Print), 2092-7622 (Online)

computationally time-consuming method (Shinozuka *et al.* 2003). Thus, development of fragility curves using nonlinear analysis (NA) is expensive; computationally time consuming and sometimes impractical particularly when complex systems are analyzed. Hence, soft computing techniques such as artificial neural networks (ANNs) seem to be good alternates, due to their capability in reducing the number of analysis in parametric studies (Hasanzadehshooiili *et al.* 2012). As a function of abstraction of the biologic neural structure, ANNs are powerful data analysis and pattern recognition tools. They are particularly able to solve problems which are too complex to be modeled with the aid of traditional procedures and classical mathematics (Adeli 2001). ANNs are also capable to capture and represent complex linear and nonlinear relationships between inputs and outputs (Perlovsky 2001). Despite neural estimating techniques are feasible to be implemented, it is noteworthy to mention that a deep attention is necessary to achieve reliable results (Kalantari and Razzaghi 2015).

In this study a methodology based on nonlinear response history analysis and ANN is proposed. To this end, seismic performances of different pre-1990 RC bridges are investigated using NA. Furthermore, MLP neural network was carried out in order to predict the seismic performances of the bridges. Finally results of NA and ANNs were used for probabilistic seismic safety evaluation of RC bridges.

2. Numerical analysis

2.1 Bridge models

In order to investigate the seismic performances of the bridges, different existing bridge attributes were adopted considering the column height, mechanical properties of concrete and yield stress of the steel reinforcement. It should be noted that all of the selected bridges were designed and constructed before 1990s. The geometric specifications of the selected bridges are indicated in Table 1. Several researchers (Priestley 1996, Avsar *et al.* 2011) are mentioned that the skew angle is one of the most important structural attributes of the highway bridges affecting their seismic performance considerably. However, based on the analysis of bridge inventory in this study, Mosleh (Mosleh 2016c) found that most of the selected bridges have skew angles less than 5°, therefore the effect of skew angle is eliminated in this study. Three-dimensional models were prepared using SAP 2000 (Computers and Structures Inc. 2009) software. As indicated in Fig. 1, structural components including superstructure and substructure are considered to create three-dimensional analytical structural model. The superstructure elements are expected to remain in the elastic range of behavior under the seismic load applied. The superstructure is composed of decks, girders, diaphragms, asphalt, parapets, and sidewalks. Span length for all selected bridges are 20 m, and bridge width is 12 m. Decks and diaphragms are modeled utilizing shell elements. Link elements are employed to model elastomeric bearings located between

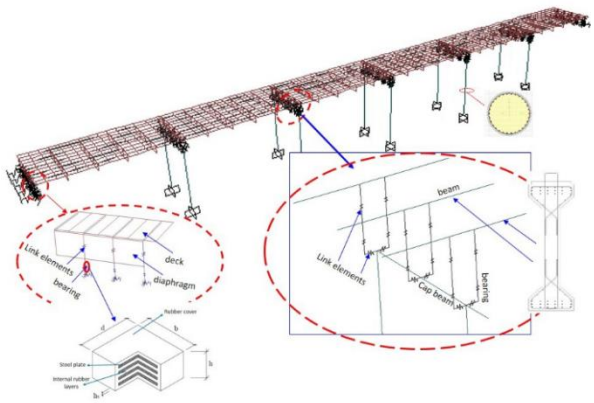

Fig. 1 Three-dimensional finite-element model using SAP2000

the substructure and superstructure without any dowel or connecting devices. The column, girders, piles, and cap beams are modeled using frame elements having six degrees of freedom at each node. The models include different bridge lengths and column heights. The cap beam is a rectangular element of 1.9 by 2.0 m, which is suported by circular columns have a diameter of 1.3-1.4 m. Each column has 30 longitudinal bars with a diameter of 20 and 18 mm spiral hoops spaced at 200 mm. Abutments and backfill soil are modeled as elastic spring in the longitudinal and transversal directions as proposed by Caltrans (2013). Rigid elements are utilized at the rigid zone of the cap beam, column, and superstructure end connections.

A bilinear approximation of the force-deformation could be employed to express the abutment longitudinal response analysis. Expansion gap including a realistic value for the embankment fill response is a factor which impacts the bilinear demand consisted of the effective abutment stiffness. Taking into account the Caltrans recommendation Caltrans (2013), the initial stiffness K_i is considered as 14.35 KN/mm/m according to the force deflection results from large- scale abutment testing (Maroney 1995, Shamsabadi 2007, Stewart *et al.* 2007). The initial abutment stiffness could be derived in terms of the back-wall height of the abutment as

$$K_{abut} = K_i w_a (\frac{h_a}{1.7}) \quad (1)$$

where h_a and w_a are the height and width of the back-wall for seat abutment, respectively.

Column bents are fixed at the bottom and soil-structure interaction is neglected. Based on Priestley *et al.* (1996) recommendation, lateral and vertical stiffness of the elastomeric bearings are modeled utilizing a spring. Shear bearing stiffness could be determined as

$$K_v = \frac{GA}{h} \quad (2)$$

where G is the shear modulus of the rubber (taken as *1 MPa*), A is gross rubber area, and h is total rubber height. Vertical bearing stiffness is adjusted as

Table 1 Structural attributes for the bridge samples

Column Height (h_{col}), (m)	Column sections	Column Diameters (m)	Longitudinal steel ratio (%)	Number of spans	Total Bridge length (m)	Concrete strength (f_c), (MPa)	Steel yield stress (f_y), (MPa)
10.5-21	Circular	1.3-1.4	0.91-1.06	6-7	120-140	20-30	300-400

$$K_z = \frac{6GAKS^2}{(6GS^2 + K)h} \quad (3)$$

where K is the rubber bulk modulus, and S is the shape factor.

The mass and stiffness proportional Rayleigh damping coefficient for the first two modal periods are calculated for the response history analysis of the bridges (Aviram *et al.* 2008). In order to assess the seismic vulnerability of the bridges, nonlinear analysis with direct integration, including P-delta effects, are taken into account in two orthogonal directions.

It is noteworthy to remark that nonlinear stress-strain relationship of concrete and steel can be employed to directly obtain the nonlinear behavior of the structure; therefore reliability of nonlinear bridge member depends on the accuracy of the material properties considered. To model reinforcing steel bars, bilinear steel material model with the kinematic hardening behavior is used due to the approach presented in the Caltrans provisions (Caltrans 2013). Nominal yield strain (ε_y) and expected yield strain (ε_{ye}) are determined as 0.0021 and 0.0013, respectively. The ultimate tensile strain (ε_{su}) depending on bar size is considered as 0.12. Various stress-strain relationships were developed for the confined concrete by previous researches (Kent and Park 1971, Bažant and Bhat 1976, Sheikh and Uzumeri 1980, Mander *et al.* 1988). Some of the suggested methods have limitation in the range of condition (e.g., circular or triangular section), however the method proposed by Mander *et al.* (1988) can be employed for all section shapes and all level of confinement. Therefore to define stress-strain relationships method proposed by Mander *et al.* (1988) considered in this study.

2.2 Ground motion

An appropriate selection of the earthquake ground motions plays a key role in developing reliable fragility curves.

The important effect of the seismic intensity measures (IM) of the ground motions on bridge fragility curves is undeniable. In fact, a specific method cannot be presented for deciding on the selection of the optimal intensity measure used in fragility analysis. Different ground motion intensity measures (such as PGA, PGV, PGD and ASI (acceleration spectral intensity)) can be employed to identify the seismic hazard level of earthquake ground motions. However, there is lack of agreement on the most suitable IM in order to develop fragility curves. Seismic intensity measures can be generally categorized into two groups, calculating intensity measures directly from ground motion records and obtaining IMs utilizing response spectrum of the ground motion for certain range of periods. PGA, as a representative of the first group, is

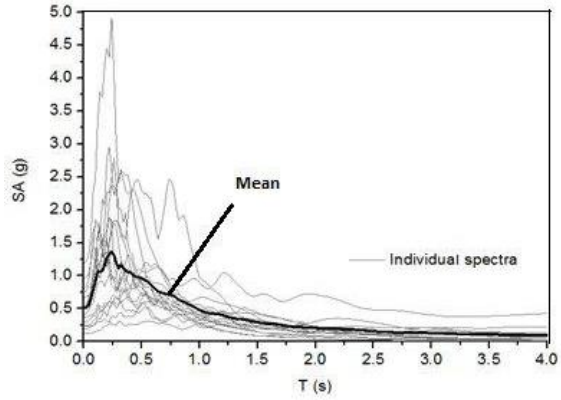

Fig. 2 Response spectra of the selected ground motions (5% damping)

the most commonly used intensity measure for bridge fragility curves (Agrawal *et al.* 2011, Brandenberg *et al.* 2011, Torbol and Shinozuka 2012, 2014, Billah and Alam 2015). Tavares *et al.* (2012) assessed the seismic vulnerability of typical as built highway bridges in eastern Canada through the development of fragility curve by employing PGA as an intensity measurement. In the study of Seo and Linzell (2012) fragility curves were generated by utilizing the seismic performance characteristics of a horizontally curved steel bridge with PGA being selected as an earthquake intensity indicator measure. On the other hand, several researchers argue that spectral acceleration at certain periods are the most appropriate since this method tends to reduce uncertainty in the demand model (Stefanidouand and Kappos 2017). The use of Sa, as an intensity measure, is recommended to quantify the collapse vulnerability of substandard RC bridge piers rehabilitated with different repair jackets under aftershock cascading events (Fakharifar *et al.* 2015).

Accounting with the appropriate level of correlation between the hazard level of the ground motion and the degree of a constant seismic damage in the bridge is one of the most important principles in selecting the appropriate intensity measure. Hence, the reliability of fragility curves is proportional to the level of correlation with the seismic damage and the selected intensity measure.

In this study, PGA is considered as an intensity indicator measure. The response spectra and mean value of the selected earthquake ground motions with a 5% damping ratio are depicted in Fig. 2. Two horizontal orthogonal components are considered in the nonlinear response history analysis Mosleh *et al.* (2016b).

In order to generate fragility curves, earthquake ground motions are collected from pacific earthquake engineering research (PEER) strong motion databases (http://peer.berkeley.edu/smcat/). The distribution of ASI versus PGA of the accelerograms was assessed in order to select the ground motions. For the ground motion

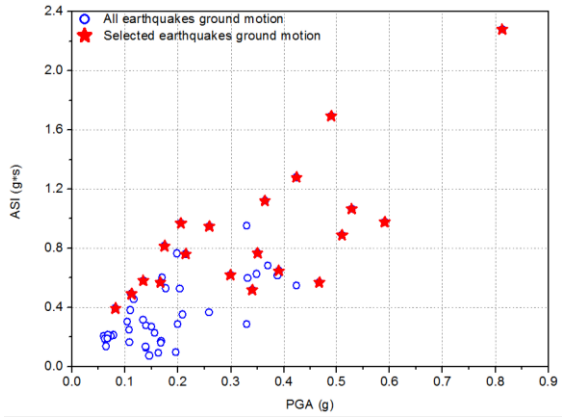

Fig. 3 Final selection of ground motions

selection, a suite of 60 earthquake ground motions were selected. Fig. 3 shows the distribution of PGA versus ASI of the selected 60 ground motions. There is not a uniform distribution for the intensity measures among the selected ground motions. Accelerograms with low intensities induce limited seismic damages on the bridges, and a small number of ground motions display high intensities. Accordingly, it was found time consuming to employ all of the selected 60 ground motions for response history analysis. Therefore, a reduced set of data of ground motions due to different levels of PGA was considered based on the study of Mosleh (2016c). A total of 20 unscaled ground motions were selected. Some of the features and characteristics of the ground motions selected are presented in Table 2. In this table, *d* represents the epicenteral distance. All bridges are considered recorded on hard soil, for what soil flexibility at the bridge foundations are not taken into account in the analytical models.

It should be noted that the following criteria were considered to select the convenient earthquake records:

- All of the selected bridges are rested on hard soils. Therefore, ground motion records were selected from sites having V_s≥360 m/s.
- Ground motions having PGA≥0.1 g
- Moment magnitude, Mw, is greater than 5.0
- Far fault earthquakes are taking into account.
- The frequency contents of the selected records were appropriate for dynamic excitation of the selected bridges.

3. Neural prediction

Artificial neural networks (ANNs), are recently drawn remarkable attention in variety of engineering applications. There are different types of artificial neural networks. The multi-layer perceptron (MLP), radial basis function network (RBFN), the probabilistic neural network (PNN), the cascade correlation neural network (Cascor) and the learning vector quantization (LVQ) are some of the popular neural network architectures (Rafiq*et al.* 2001, Razzaghi and Mohebbi 2011). However, RBF and MLP are the most widely used in engineering problems (Kalantari and Razzaghi 2015). In present study the MLP neural networks are implemented.

3.1 MLP neural networks

The theoretical background of MLP neural networks is presented in many research articles (Rafiq *et al.* 2001, Waszczyszyn and Bartczak 2002, Graham *et al.* 2006, Lagaros and Fragiadakis 2007, Mehrjoo *et al.* 2008, Elshafey *et al.* 2010). The MLP neural networks include a single input layer, one or more hidden layer(s) and an output layer. Each layer includes one or more artificial neuron(s). All neurons in a MLP network are fully connected to the neurons of the neighboring layer; however neurons within a same layer are not connected together. The path connecting neurons *i* and *j* is associated with synaptic strength, w_{ij}. The particular neuron j sums up all the input coming to it as follows

$$x_j = \sum_{i=1}^{m} w_{ij} O_i \tag{4}$$

where O_i denotes the output of the neuron *i*. It should be noted that the activation of each neuron depends on an activation function and a threshold value. Hence x_j would be an output of neuron *j* provided that the neuron is activated. Generally various activation functions are available for MLP neural networks. In this study the sigmoid function is used as follows

$$S(x_j) = \frac{1}{1+e^{(x_j-\theta_j)}} \tag{5}$$

where θ_j is the threshold value of the neuron *j*.

The information distributes from input layer to the hidden layer(s). Then the hidden layer passes the information onto the output layer. Such a neural network is called a feed forward neural network. A MLP neural network requires a training algorithm for learning a relationship between input and output vectors. One of the most common training algorithms is back propagation algorithm. It minimizes the error function by using the gradient search method. The error function is the mean square difference of the desired and the predicted output. The error can be mathematically describes as follows

$$E_T(T|w,A) = \frac{1}{2}\sum_{m}(y(x^m;w,A)) - t^m)^2 \tag{6}$$

where *T* is the training set having m input-target pairs ($T=[x^m,t^m]$), A denotes the architecture of ANN, *w* is the weight parameter assigned to the neuron connections. $y(x^m;w,A)$ is defined as mapping between input vector x^m and output vector *y*.

In order to minimize the error function and determine the optimum weight parameter, iterative algorithms are used as follows

$$W^{(k+1)} = W^k + \Delta W^k \tag{7}$$

$$\Delta W^k = -\eta \frac{\partial E_T}{\partial W^k} \tag{8}$$

The superscript *k* is an iteration counter and η is a constant learning rate and $\eta \in [0,1]$.

In the present work, the MLP neural networks are

Table 2 Important features of the selected ground motions

	Earthquake	Station	Year	M_w	d (Km)	PGA (g)
1	Chi-Chi	CWB 99999 TCU015	1999	7.62	101.62	0.1125
2	Chi-Chi	CWB 9999917 NSY	1999	7.62	63.29	0.1348
3	Chi-Chi	CWB 9999917 ALS	1999	7.62	37.83	0.1748
4	Chi-Chi	CWB 99999 TCU070	1999	7.62	47.86	0.2058
5	Chi-Chi	CWB 99999 CHY029	1999	7.62	39.70	0.2595
6	Chi-Chi	CWB 99999 TCU047	1999	7.62	86.39	0.3643
7	Chi-Chi	CWB 99999 TCU095	1999	7.62	95.70	0.5283
8	Chi-Chi	CWB 99999 CHY042	1999	7.62	59.80	0.0823
9	Northridge	USC 90015 LA - Chalon Rd	1994	6.69	14.92	0.2148
10	Northridge	CDMG 24688 LA - UCLA Grounds	1994	6.69	18.62	0.3908
11	Northridge	CDMG 24400 LA - Obregon Park	1994	6.69	39.39	0.4673
12	Northridge	CDMG 24278 Castaic - Old Ridge Route	1994	6.69	40.68	0.4898
13	Northridge	USC 90014 Beverly Hills - 12520 Mulhol	1994	6.69	16.27	0.5102
14	Northridge	CDMG 24538 Santa Monica City Hall	1994	6.69	22.45	0.5908
15	Sanfernando	CDMG 24278 Castaic - Old Ridge Route	1971	6.61	25.36	0.2994
16	Whittier Narrows	CDMG 14403 LA - 116th St School	1987	5.99	21.26	0.3408
17	Capemendocino	CDMG 89509 Eureka - Myrtle & West	1992	7.01	53.34	0.1668
18	Capemendocino	CDMG 89324 Rio Dell Overpass - FF	1992	7.01	22.64	0.4244
19	Tabas	9102 Dayhook	1978	7.40	20.63	0.3505
20	Tabas	9101 Tabas	1978	7.40	55.24	0.8128

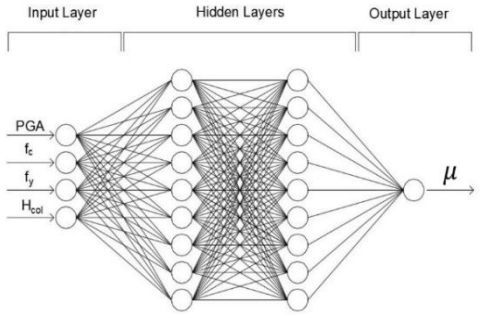

Fig. 4 Proposed MLP structure

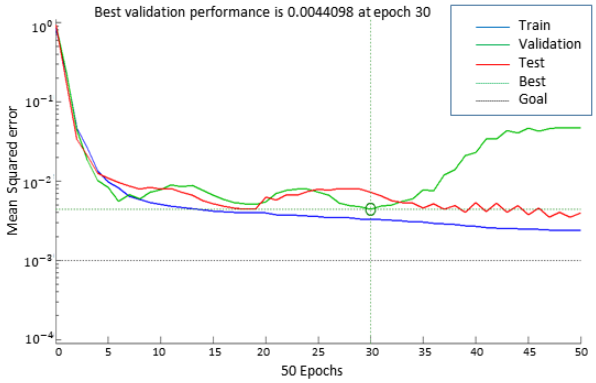

Fig. 5 Performance curve of the selected neural network

employed for the assessment of seismic performance of highway bridges. Multi-layered perceptron neural networks utilized herein consist of a single input and output layer and two hidden layers. As input vectors, PGA, f_C, f_Y and h_{COL} are considered and the displacement ductility ratio is considered as an output of the network. Fig. 4 illustrates a schematic structure of MLP neural network applied in this study.

3.2 Structure of MLP neural network

In order to select the optimum structure for neural networks the mean squared error (MSE) and the squared correlation coefficient (R^2) are considered as criteria. MSE and R^2 can be determined by utilizing the following equations

$$MSE = \frac{1}{n}\sum(\hat{y}_t - y_t)^2 \tag{9}$$

$$R^2 = 1 - \frac{\sum(\hat{y}_t - y_t)^2}{\sum \hat{y}_t^{\,2}} \tag{10}$$

where n is the pattern, $\hat{y}_t$ is the output value and y_t is the target value.

In order to train and construct the ANN model, the back propagation (BP) is applied. Moreover, 70% of the results of the numerical analysis were selected for training the ANNs. To test the reliability of ANNs, 15% of the results were used and the remaining results were utilized to validate the proposed ANN model. Furthermore, the sigmoid transfer function is employed for each of the ANNs.

Generally there is no unique reliable method for deciding the number of hidden layers and their neural units required for a particular problem. To select the best configuration, the decision may made based on few trials (Mukherjee and Biswas 1997). Hence, in this study several structures of MLP neural networks were examined and the structure with the minimum MSE and the maximum coefficient of correlation was elected as the most relatively proper neural network. It should be noted that the selected neural network had two hidden layers with nine

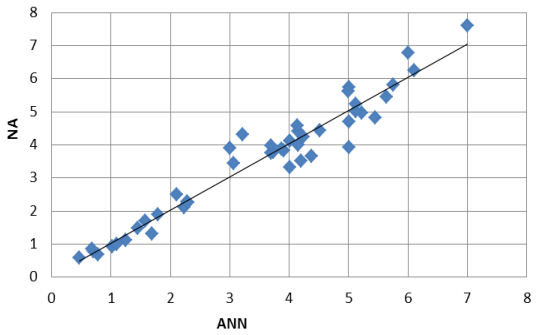

Fig. 6 Comparison of NA results with neural predictions for ductility ratios of the bridges (μ)

neurons at each hidden layer. The MSE of the selected structure was 0.00378 and its R^2 was 0.85. The performance curve of the selected neural network is indicated in Fig. 5. Moreover, Fig. 6 indicates the ANN predictions versus results of NA for validation samples.

4. Development of fragility curves

A fundamental requirement for seismic safety evaluation of existing bridges is the ability of quantifying the potential for damage as a function of the severity of strong ground motion. Fragility functions can relate the probability of occurring or exceeding from a particular limit state to the level of seismic hazards (e.g., PGA). Such a probabilistic function can be expressed as follows

$$P_f = P[(\frac{S_d}{S_c} \geq 1 | IM)] \quad (11)$$

where P_f is the probability of reaching or exceeding a particular damage state, IM is the ground motion intensity measure, S_d is structural demand and S_c is capacity of the bridge.

The cumulative lognormal distribution is mathematically convenient for characterizing the uncertainties and randomness associated with the seismic performance of a particular structure (Straub and Der Kiureghian 2008, Hancilar *et al.* 2013). Hence, during the past decades, several researches assumed that the earthquake damage distribution can be represented by the cumulative standard lognormal function (Kircher *et al.* 1997, Shinozuka *et al.* 2000, Choi *et al.* 2004, Hancilar *et al.* 2013, Razzaghi and Eshghi 2014). In this study, cumulative standard lognormal function was considered for earthquake damage distribution of the bridges. Hence, the Eq. (15) can be rewritten as follows

$$P_f = P[(\frac{S_d}{S_c} \geq 1 | IM)] = \Phi[\frac{1}{\beta} ln(\frac{S_d}{S_c})] \quad (12)$$

where Φ is the standard normal distribution function and β is the logarithmic standard deviation of variables.

4.1 Capacity limit states

In order to calculate the structural capacities, appropriate limit states should be defined. During the recent years several quantitative and/or qualitative damage states have been proposed and employed. HAZUS (FEMA 2003) provided five qualitative damage states (see Table 3). For member and structure responses, qualitative and quantitative limit states were employed based on the study of Priestley *et al.* (1996). In the study of Kawashima (2000), a quantitative strain and ductility limit corresponding to the three damage levels were proposed for the seismic damage assessment. Kowalsky (2000) specified two damage limit states for the seismic damage assessment namely: "serviceability" and "damage control". To develop analytical fragility curves, three damage states were considered by Avsar and Yakut (2012). Four limit states were defined for evaluation of the seismic damages due to the study of Jara *et al.* (2013). Hose *et al.* (2000) utilized five limit states and performance level for the seismic damage of the bridges based on the crack width. Displacement ductility ratios of the columns have been implemented by several researchers for fragility analysis of the bridges (Hwang *et al.* 2001, Mosleh *et al.* 2015, Mosleh *et al.* 2016b). The damage states considered in the present study are adopted from Hwang *et al.* (2001). The definition of limit states in the present study is indicated in Table 3. As indicated in Table 3, five damage states, which are equivalent to those defined by HAZUS, are defined for seismic vulnerability assessment of highway bridges.

Table 3 Description of damage states, adopted from HAZUS (FEMA 2003) and Hwang *et al.* (2001)

Limit state	Quantitative definition	Equivalent HAZUS Damage state	Qualitative description
LS0	$\mu<\mu_1$	DS1 (no damage)	No damage
LS1	$\mu_1\leq\mu_1<\mu_y$	DS2 (slight/minor)	Minor spalling at the column, abutments, hinges or deck (damage requires no more than cosmetic repair). Minor cracks at shear keys.
LS2	$\mu_y\leq\mu<\mu_2$	DS3 (moderate)	Moderate cracking and spalling of any column (column structurally still sound), moderate movement of the abutment (<0.05m), extensive damage to shear keys.
LS3	$\mu_2\leq\mu<\mu_c$	DS4 (extensive)	Extensive damage to columns. Unsafe columns without collapse, significant residual movement at connections, vertical offset of the abutment.
LS4	$\mu\geq\mu_c$	DS5 (collapse)	Collapse of any column. Tilting of substructure due to the geotechnical aspects. Deck collapse.

In Table 3, μ denotes the displacement ductility ratio which can be calculated by the following equation

$$\mu = \frac{\Delta}{\Delta_1} \tag{13}$$

where Δ is the maximum relative displacement of the top of the columns due to a particular seismic event and Δ_1 is relative displacement at the top of a column at the corresponding limit state 1 (as indicated in Fig. 7) and can be determined as follows

$$\Delta_1 = \frac{1}{3}\varphi_1 L^2 \tag{14}$$

where L is the distance from the plastic hinge to the point of contra-flexure and φ_1 is the curvature corresponding to the relative displacement of a column when the vertical reinforcing bars at the bottom of the column reaches the first yield. The displacement ductility ratio corresponding to the first yield point, μ_1, is always equal to 1. The second damage state, μ_v, denotes the yield displacement ductility ratio, can be calculated using the following equation (See Fig. 7)

$$\mu_y = \frac{\Delta_y}{\Delta_1} = \frac{1}{3}\frac{\varphi_y L^2}{\Delta_1} \tag{15}$$

The equivalent curvature (φ_y) corresponds to the relative displacement of the column when the vertical reinforcing bars at the bottom of the column reach the yield point. φ_y is obtained by extrapolating the line joining the origin and the point corresponding to the first yielding point of a reinforcing bar up to the nominal moment capacity M_n [108, 124]. Eq. (16) gives the curvature φ_y, where M_y and φ_{y1} are the moment and curvature at first yielding of a vertical reinforcing bar. The curvature φ_y and M_y are the curvature and moment at yielding of a vertical reinforcing bar, given by Eq. (17).

$$\varphi_y = \frac{M_n}{M_y}\varphi_{y1} \tag{16}$$

$$\varphi_y = \frac{M_n}{EI_e} \tag{17}$$

The displacement ductility corresponding to the third damage state, which is nominated: μ_3, can be calculated as follows (Hwang *et al*. 2001)

$$\mu_2 = \frac{\Delta_2}{\Delta_1} = \frac{\Delta_y + \theta_p(L - \frac{L_p}{2})}{\Delta_1} \tag{18}$$

as which θ_p and L_p denote the hinge rotation and the plastic hinge length, respectively. The plastic hinge rotation can be determined as

$$\theta_p = (\varphi_2 - \varphi_y)L_p \tag{19}$$

where φ_2 denotes the curvature of a column when ε_c=0.002 or ε_c=0.004 for the columns with or without lap splices, respectively (Hwang *et al*. 2001). In this study the effect of lap splice is not considered therefore ε_c=0.004. Several

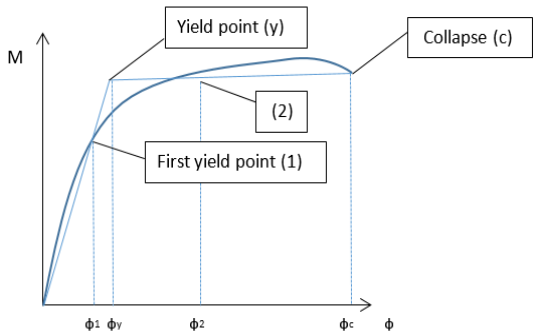

Fig. 7 Definition of limit states on the moment-curvature plot of a bridge pier

relations are available for calculating plastic hinge length (Bae and Bayrak 2008, Bayrak and Sheikh 2001, Priestly *et al*. 1996). Although there is some scatter among the plastic hinge lengths calculated by different relations, the estimated limit state is not noticeably sensitive to the plastic hinge length. In this study the plastic hinge length is calculated according to Priestley *et al.* (1996) as follows

$$L_p = 0.08L + 0.022\, f_{ye} d_{bl} \geq 0.044\, f_{ye} d_{bl} \tag{20}$$

where f_{ye} denotes the yield strength of the reinforcing bars and d_{bl} denots the diameter of the longitudinal reinforcing bars. Finally, the forth damage state which is nominated μ_c can be calculated *as* μ_c=μ_2+3 (FHWA 1995, Hwang *et al.* 2001).

4.2 NA based fragility curves

Totally, 306 bridge-earthquake analyses were performed. Results of these numerical analyses were used for development of seismic fragility curves.

Lognormal distribution functions were employed as a mathematical expression of fragility curves. Peak ground acceleration of the strong ground motions were considered as intensity measure of the earthquakes. Squared correlation coefficient of this set of fragility curves are in the range of R^2=0.79-0.93 which is reasonable for engineering purposes (O'Rourke and So 2000, Razzaghi and Eshghi 2014). Fig. 8 presents NA based fragility curves for different limit states. It should be noted that the fragility curves illustrated in Fig. 8 belong to all of the bridges with various mechanical properties of reinforcements. NA based fragility curves for certain values of reinforcement yield stress (f_y) had significant low correlation coefficients (generally less than 0.7). The number of data is very important in every statistical or probabilistic problem. In other words, the accuracy of results in probabilistic methods is highly dependent to the number of available data. Hence, the insufficient number of analyses, may lead to unreasonable scatter in the results of fragility analyses (O'Rourke and So 2000, Razzaghi and Eshghi 2014). Hence, the insufficient number of bridge-earthquake cases for certain reinforcement yield stresses can be considered as one of the most important reasons for inappropriate coefficients of correlations. In other words, development of appropriate NA based fragility curves for bridges with

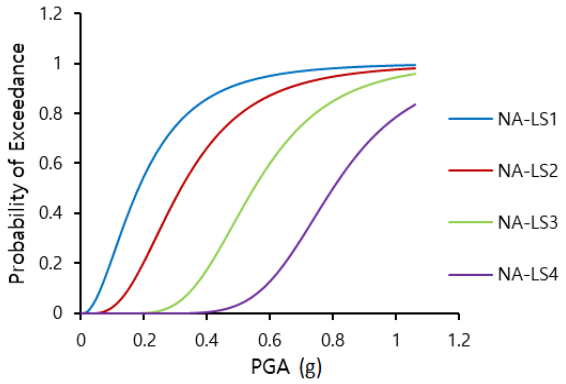

Fig. 8 Fragility curves corresponding to four damage limit states for three groups of classification

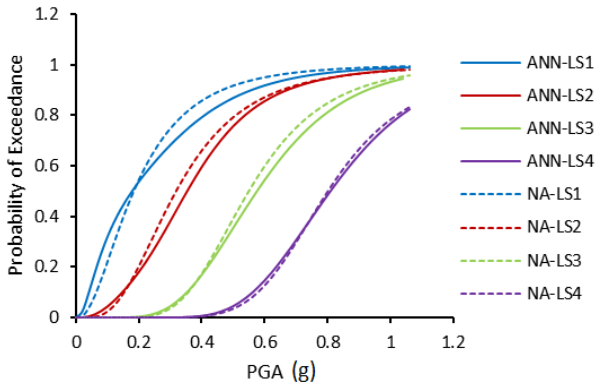

Fig. 9 Fragility curves created by both ANN-based and NA-based approaches

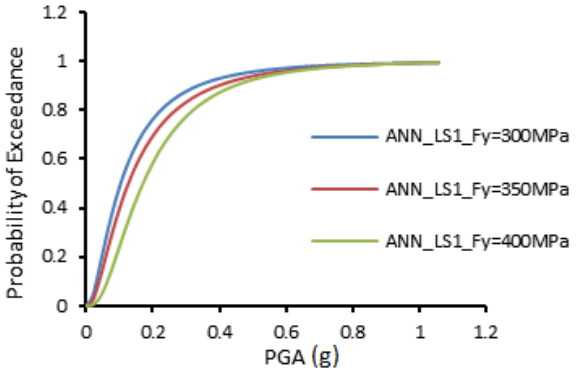

(a) LS1

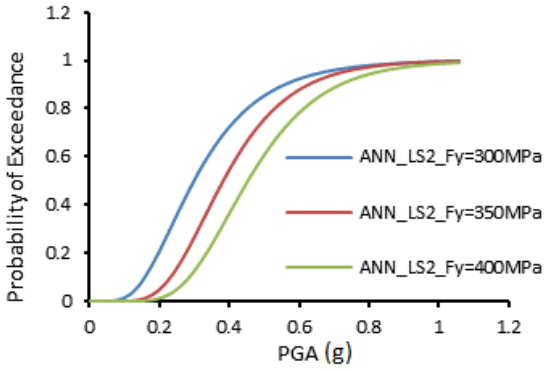

(b) LS2

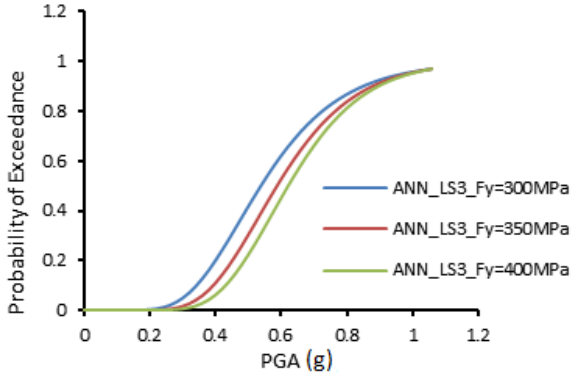

(c) LS3

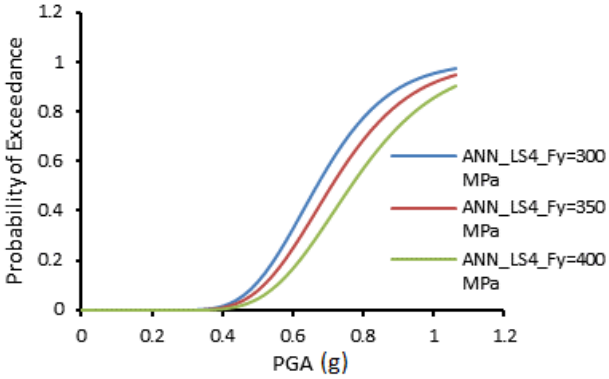

(d) LS4

Fig. 10 ANN-based fragility curves using interpolation method

certain values of f_y requires remarkable number of numerical analyses.

4.3 ANN based fragility curves

As expressed before, conventional NA based method is computationally time consuming, expensive and sometimes impossible because of convergence problems. In such a case soft computing techniques may be useful. Hence, in the present study, ANN predictions were used to derive fragility functions. To this end, the trained neural network was employed to simulate new bridge-earthquake cases and predict their seismic performances. Hence, the total number of 600 neural samples were created and used to develop ANN based fragility curves. Fig. 9 indicates the ANN based fragility curves for all of the bridges comparing to NA based ones. As illustrated in Fig. 9, NA based and ANN based fragility curves are somewhat different for LS1, LS2 and LS3 but very similar in LS4. It should be noted that squared correlation coefficients of this ANN based fragility curves are in the range of R^2=0.85-0.96.

In addition to the above mentioned fragility curves, ANN based fragility curves were developed for bridges with certain values of reinforcement yield stress (f_y=300, 350 and 400 MPa). Squared correlation coefficients of this set of fragility curves are in the range of R^2=0.82-0.94. The ANN based fragility curves for bridges with certain values of f_y are shown in Fig. 10. As indicated in Fig. 10, the yield

stress of reinforcement plays a considerable role in seismic fragility of RC bridges. In other words, it can be considered as one of the most important sources of uncertainty in probabilistic seismic performance assessment of the bridges.

5. Conclusions

A methodology based on numerical analysis and artificial neural networks was presented for the development of seismic fragility curves of RC bridges. Nonlinear dynamic response history analyses were performed by using appropriate records of strong ground motions. To consider uncertainties involved in fragility analysis of RC bridges, 306 bridge-earthquake cases were numerically analyzed. Based on the results of numerical analyses, the fragility curves were developed. Meanwhile, artificial neural networks were employed to predict seismic performances of RC bridges. Herein, MLP neural networks were employed. The proper structure of ANN was selected by minimizing the MSE and maximizing R^2.

Results of this study revealed that MLP neural networks are useful tools to predict the seismic performance of RC bridges. Hence, ANN can be used to develop seismic fragility curves for bridges. It was shown that by generating the new reliable cases, ANN can produce the strong database. Thus, it would be capable of developing fragility curves for special cases in which NA is weak. For instance, in the present study NA was not capable of developing reasonable fragility curves in terms of f_y. Whilst, by using ANN, appropriate fragility curves were developed for various yield stresses.

Furthermore, ANN-based fragility curves which developed in terms of f_y showed that the grade of the reinforcing bar can considerably change the fragility of RC bridges. In other words, the yield stress of the bars can be considered as one of the important sources of uncertainty in seismic fragility of RC bridges.

References

Adeli, H. (2001), "Neural networks in civil engineering: 1989-2000", *Comput. Aid. Civil Infrastr. Eng.*, **16**(2), 126-142.

Agrawal, A., Ghosn, M., Alampalli, S. and Pan, Y. (2011), "Seismic fragility of retrofitted multispan continuous steel bridges in New York", *J. Bridge Eng.*, **17**(4), 562-575.

Arslan, M.H. (2010), "Predicting of torsional strength of RC beams by using different artificial neural network algorithms and building codes", *Adv. Eng. Softw.*, **41**(7), 946-955.

ATC (1991), "Seismic vulnerability and impact of disruption of lifelines in the Coterminous United States", Report No. ATC-25, Applied Technology Council, Redwood City, CA.

Aviram, A., Mackie, K.R. and Stojadinović, B. (2008), "Guidelines for nonlinear analysis of bridge structures in California", Pacific Earthquake Engineering Research Center, College of Engineering University of California, Berkeley, PEER Report 2008/03.

Avsar, O. and Yakut, A. (2012), "Seismic vulnerability assessment criteria for RC ordinary highway bridges in Turkey", *Struct. Eng. Mech.*, **43**(1), 127-145.

Avsar, O., Yakut, A. and Caner, A. (2011), "Analytical fragility curves for ordinary highway bridges in Turkey", *Earthq. Spectra*, **27**(4), 971-996.

Bae, S. and Bayrak, O. (2008), "Plastic hinge length of reinforced concrete columns", *ACI Struct. J.*, **105**(3), 290.

Banerjee, S. and Shinozuka, M. (2007), "Nonlinear static procedure for seismic vulnerability assessment of bridges", *Comput. Aid. Civil Infrastr. Eng.*, **22**(4), 293-305.

Bayrak, O. and Sheikh, S.A. (2001), "Plastic hinge analysis", *J. Struct. Eng.*, **127**(9), 1092-1100.

Bažant, Z.P. and Bhat, P.D. (1976), "Endochronic theory of inelasticity and failure of concrete", *J. Eng. Mech. Div.*, **102**(4), 701-722.

Billah, A. and Alam, M.S. (2015), "Seismic fragility assessment of concrete bridge pier reinforced with superelastic shape memory alloy", *Earthq. Spectra*, **31**(3), 1515-1541.

Billah, A.M. and Alam, M.S. (2016), "Performance-based seismic design of shape memory alloy-reinforced concrete bridge piers I: Development of performance-based damage states", *J. Struct. Eng.*, **142**(12), 04016140.

Billah, A.M. and Alam, M.S. (2016), "Performance-based seismic design of shape memory alloy-reinforced concrete bridge piers. I: Development of performance-based damage states", *J. Struct. Eng.*, **142**(12), 04016140.

Billah, A.M., Alam, M.S. and Bhuiyan, M.R. (2012), "Fragility analysis of retrofitted multicolumn bridge bent subjected to near-fault and far-field ground motion", *J. Bridge Eng.*, **18**(10), 992-1004.

Brandenberg, S.J., Zhang, J., Kashighandi, P., Huo, Y. and Zhao, M. (2011), "Demand fragility surfaces for bridges in liquefied and laterally spreading ground", Pacific Earthquake Engineering Research Center, College of Engineering University of California, Berkeley, PEER Report 2011/0.

Caltrans (2013), Seismic Design Criteria Version 1.7, California Department of Transportation, Sacramento, CA.

Choi, E., DesRoches, R. and Nielson, B. (2004), "Seismic fragility of typical bridges in moderate seismic zones", *Eng. Struct.*, **26**(2), 187-199.

Computers and Structures Inc. (2009), "Integrated finite element analysis and design of structures basic analysis reference manual", Computers and Structures, Berkeley, CA, USA

Elshafey, A.A., Haddara, M.R. and Marzouk, H. (2010), "Damage detection in offshore structures using neural networks", *Marine Struct.*, **23**(1), 131-145.

Fakharifar, M., Chen, G., Dalvand, A. and Shamsabadi, A. (2015), "Collapse vulnerability and fragility analysis of substandard RC bridges rehabilitated with different repair jackets under post-mainshock cascading events", *Int. J. Concrete Struct. Mater.*, **9**(3), 345-367.

FEMA (2003), HAZUS-MH MR1: Technical Manual, Vol. Earthquake Model, Federal Emergency Management Agency; Washington D.C.

FHWA (1995), Seismic Retrofitting Manual for Highway Bridges Publication No.FHWA-RD-94-052, Office of Engineering and Highway Operations R&D, Federal Highway Administration; McLean, VA.

Graham, L.D., Forbes, D.R. and Smith, S.D. (2006), "Modeling the ready mixed concrete delivery system with neural networks", *Auto. Constr.*, **15**(5), 656-663.

Hancilar, U., Taucer, F. and Corbane, C. (2013), "Empirical fragility functions based on remote sensing and field data after the 12 January 2010 Haiti earthquake", *Earthq. Spectra*, ***29***(4), 1275-1310.

Hasanzadehshooiili, H., Lakirouhani, A. and Šapalas, A. (2012), "Neural network prediction of buckling load of steel arch-shells", *Arch. Civil Mech. Eng.*, **12**(4), 477-484.

HAZUS (1997), MH 2.0, Technical Manual, Federal Emergency

Management Agency, Washington, DC.
Hose, Y., Silva, P. and Seible, F. (2000), "Development of a performance evaluation database for concrete bridge components and systems under simulated seismic loads", *Earthq. Spectra*, **16**(2), 413-442.
Huo, Y. and Zhang, J. (2012), "Effects of pounding and skewness on seismic responses of typical multispan highway bridges using the fragility function method", *J. Bridge Eng.*, **18**(6), 499-515.
Hwang, H., Liu, J. and Chiu, Y. (2001), "Seismic fragility analysis of highway bridges", Center for Earthquake Research and Information, The University of Memphis, MAEC RR-4 Project.
Jara, M., Jara, J. and Olmos, B. (2013), "Seismic energy dissipation and local concentration of damage in bridge bents", *Struct. Infrastr. Eng.*, **9**(8), 794-805.
Kalantari, Z. and Razzaghi, M. (2015), "Predicting the buckling capacity of steel cylindrical shells with rectangular stringers under axial loading by using artificial neural networks", *Int. J. Eng.-Tran. B: Appl.*, **28**(8), 1154.
Kawashima, K. (2000), "Seismic design and retrofit of bridges", *Bull. NZ Soc. Earthq. Eng.*, **33**(3), 265-285.
Kent, D.C. and Park, R. (1971), "Flexural members with confined concrete", *Automated Vehicles Symposium*, San Francisco, July.
Kircher, C.A., Nassar, A.A., Kustu, O. and Holmes, W.T. (1997), "Development of building damage functions for earthquake loss estimation", *Earthq. Spectra*, **13**(4), 663-682.
Kowalsky, M.J. (2000), "Deformation limit states for circular reinforced concrete bridge columns", *J. Struct. Eng.*, **126**(8), 869-878.
Lagaros, N.D. and Fragiadakis, M. (2007), "Fragility assessment of steel frames using neural networks", *Earthq. Spectra*, **23**(4), 735-752.
Mander, J., Priestley, M. and Park, R. (1988), "Observed stress-strain behavior of confined concrete", *J. Struct. Eng.*, **114**(8), 1827-1849.
Maroney, B.H. (1995), *Large Scale Bridge Abutment Tests to Determine Stiffness and Ultimate Strength Under Seismic Loading*, University of California, Davis.
Mehrjoo, M., Khaji, N., Moharrami, H. and Bahreininejad, A. (2008), "Damage detection of truss bridge joints using Artificial Neural Networks", *Exp. Syst. Appl.*, **35**(3), 1122-1131.
Monti, G. and Nisticò, N. (2002), "Simple probability-based assessment of bridges under scenario earthquakes", *J. Bridge Eng.*, **7**(2), 104-114.
Moschonas, I.F., Kappos, A.J., Panetsos, P., Papadopoulos, V., Makarios, T. and Thanopoulos, P. (2009), "Seismic fragility curves for Greek bridges: methodology and case studies", *Bull. Earthq. Eng.*, **7**(2), 439-468.
Mosleh, A. (2016c), "Seismic vulnerability assessment of existing concrete highway Iranian bridges", Doctor of Philosophy, Aveiro University, http://hdl.handle.net/10773/17173.
Mosleh, A., Jara, J. and Varum, H. (2015), "A methodology for determining the seismic vulnerability of old concrete highway bridges by using fragility curves", *J. Struct. Eng. Geotech.*, **5**(1), 1-7.
Mosleh, A., Razzaghi, M. S., Jara, J. andVarum, H. (2016b), "Development of fragility curves for RC bridges subjected to reverse and strike-slip seismic sources", *Earthq. Struct.*, **11**(3), 517-538.
Mosleh, A., Razzaghi, M.S., Jara, J. and Varum, H. (2016a), "Seismic fragility analysis of typical Pre-1990 bridges due to near and far-field ground motions", *Int. J. Adv. Struct. Eng.*, **8**(1), 1-9.
Mosleh, A., Razzaghi, M.S., Jara, J. and Varum, H. (2018b), "Probabilistic seismic performance analysis of RC bridges", *J. Earthq. Eng.*, 1-25, doi.org/10.1080/13632469.2018.1477637.
Mosleh, A., Sepahvand, S., Varum, H., Jara, J., Razzaghi, M.S. and Marburg, S. (2018a), "Stochastic collocation-based nonlinear analysis of concrete bridges with uncertain parameters", *Struct. Infrastr. Eng. J.*, **14**(10),1324-1338.
Mukherjee, A. and Biswas, S.N. (1997), "Artificial neural networks in prediction of mechanical behavior of concrete at high temperature", *Nucl. Eng. Des.*, **178**(1), 1-11.
MuntasirBillah, A. and ShahriaAlam, M. (2015), "Seismic fragility assessment of highway bridges: a state-of-the-art review", *Struct. Infrastr. Eng.*, **11**(6), 804-832.
O'Rourke, M.J. and So, P. (2000), "Seismic fragility curves for on-grade steel tanks", *Earthq. Spectra*, ***16***(4), 801-815.
Padgett, J.E., Ghosh, J. and Dueñas-Osorio, L. (2013), "Effects of liquefiable soil and bridge modelling parameters on the seismic reliability of critical structural components", *Struct. Infrastr. Eng.*, **9**(1), 59-77.
Perlovsky, L.I. (2001), *Neural Networks and Intellect: Using Model-Based Concepts*, Oxford University Press, New York.
Priestley, M.N., Seible, F. and Calvi, G.M. (1996), *Seismic Design and Retrofit of Bridges*, John Wiley & Sons.
Rafiq, M., Bugmann, G. and Easterbrook, D. (2001), "Neural network design for engineering applications", *Comput. Struct.*, **79**(17), 1541-1552.
Razzaghi, M.S. and Eshghi, S. (2014), "Probabilistic seismic safety evaluation of precode cylindrical oil tanks", *J. Perform. Constr. Facil.*, **29**(6), 04014170.
Razzaghi, M.S. and Mohebbi, A. (2011), "Predicting the seismic performance of cylindrical steel tanks using artificial neural networks (ann)", *Acta Polytechnica Hungarica*, **8**(2), 129-140.
Sadovský, Z. and Soares, C.G. (2011), "Artificial neural network model of the strength of thin rectangular plates with weld induced initial imperfections", *Reliab. Eng. Syst. Saf.*, **96**(6), 713-717.
Seo, J. and Linzell, D.G. (2012), "Horizontally curved steel bridge seismic vulnerability assessment", *Eng. Struct.*, **34**, 21-32.
Shamsabadi, A. (2007), "Three-dimensional nonlinear seismic soil-abutment-foundation structure interaction analysis of skewed bridges", Ph.D. Dissertation, University of Southern California, Los Angeles, CA.
Sheikh, S. and Uzumeri, M. (1980), "Strength and ductility of confined concrete columns", *J. Struct. Eng.*, **106**, 1079-1102.
Shinozuka, M., Feng, M., Kim, H., Uzawa, T. and Ueda, T. (2003), "Statistical analysis of fragility curves", Report No. MCEER-03-0002, Multidisciplinary Center for Earthquake Engineering Research.
Stefanidou, S.P. and Kappos, A.J. (2017), "Methodology for the development of bridge-specific fragility curves", *Earthq. Eng. Struct. Dyn.*, **46**(1), 73-93.
Stewart, J.P., Taciroglu, E., Wallace, J.W., Ahlberg, E.R., Lemnitzer, A., Rha, C. and Salamanca, A. (2007), "Full scale cyclic testing of foundation support systems for highway bridges. Part II: Abutment backwalls", Retrieved from Los Angeles, CA.
Straub, D. and Der Kiureghian, A. (2008), "Improved seismic fragility modeling from empirical data", *Struct. Saf.*, **30**(4), 320-336.
Tavares, D.H., Padgett, J.E. and Paultre, P. (2012), "Fragility curves of typical as-built highway bridges in eastern Canada", *Eng. Struct.*, **40**, 107-118.
Torbol, M. and Shinozuka, M. (2012), "Effect of the angle of seismic incidence on the fragility curves of bridges", *Earthq. Eng. Struct. Dyn.*, **41**(14), 2111-2124.
Torbol, M. and Shinozuka, M. (2014), "The directionality effect in the seismic risk assessment of highway networks", *Struct. Infrastr. Eng.*, **10**(2), 175-188.
Waszczyszyn, Z. and Bartczak, M. (2002), "Neural prediction of buckling loads of cylindrical shells with geometrical imperfections", *Int. J. Nonlin. Mech.*, **37**(4-5), 763-775.

Whitman, R.V., Vanmarcke, E.H., de Neufville, R.L., Brennan, J., Cornell, C.A. and Biggs, J.M. (1975), "Seismic design decision analysis", *J. Struct. Div.*, **101**(5), 1067-1084.
Yazgan, U. (2015), "Empirical seismic fragility assessment with explicit modeling of spatial ground motion variability", *Eng. Struct.*, **100**(1), 479-489.

CC